Electronic Supplementary Material (ESI) for Journal of Materials Chemistry A.

Supplementary information

Homologous NiCoP@NiFeP Heterojunction Array Achieving High-Current Hydrogen Evolution for Alkaline Anion Exchange Membrane Electrolyzers

Yingxia Zhao, [a] Ming Sun, [a] Qunlei Wen, [b] Shuzhe Wang, [b] Shengbo Han, [a] Leheng Huang, [a] Gao cheng, [a] Youwen Liu[b]* and Lin Yu[a]*

Y.X. Zhao, Prof. M. Sun, S. B. Han, L. H. Huang, Gao cheng, Prof. L. Yu
[a] Key Laboratory of Clean Chemistry Technology of Guangdong Regaular Higher Education Institutions, Guangdong Provincial Key Laboratory of Plant Resources Biorefinery, School of Chemical Engineering and Light Industry, Guangdong University of Technology, Guangzhou, 510006, P. R. China
E-mail: gych@gdut.edu.cn

Q. L. Wen, S. Z. Wang, Prof. Y. W. Liu
[b] State Key Laboratory of Materials Processing and Die & Mould Technology, School of Materials Science and Engineering, Huazhong University of Science and Technology, Wuhan 430074, P. R. China
E-mail: ywliu@hust.edu.cn

Materials

All the chemicals were used as received without further purification. Cobalt chloride hexahydrate ($CoCl_2 \cdot 6H_2O$, Chemical Reagent), nickel chloride hexahydrate ($NiCl_2 \cdot 6H_2O$, Chemical Reagent) Ferric nitrate nonahydrate ($Fe(NO_3)_3 \cdot 9H_2O$, Macklin), urea (Macklin), sodium hypophosphite hydrate ($NaH_2PO_2 \cdot H_2O$, Chemical Reagent), potassium hydroxide (KOH, Macklin), RuO_2 (Aladdin), and platinum on carbon (20 wt% Pt/C, Aladdin).

Characterizations

The phase composition of the samples was identified using a PANalytical X-ray Diffractometer (X'Pert3 Powder) equipped with Cu Kα radiation in the scanning range of 10-80° (2θ). The morphology of the materials was observed on a Hitachi Su8220 scanning the field emission scanning electron microscope (FESEM) and high-resolution transmission electron microscopy (HRTEM), select area electron diffraction (SAED) pattern, and energy-dispersive spectrometer elemental mapping (EDX-mapping) were acquired on Bruker Nano

GmbH Berlin. The chemical composition and status of samples were detected by using Thermo Fisher Escalab 250Xi X-ray photoelectron spectroscopy (XPS).

Electrochemical measurements

The electrochemical measurements were conducted on an electrochemical workstation (ZAHNER ZENNIUM/IM6) using a standard tri-electrode system. Only 1 cm^2 of electrocatalyst is served as the working electrode, and graphite rod and Ag/AgCl electrode (3.5 M KCl solution) were served as counter electrode and reference electrode, respectively. The potentials measured were converted to the reversible hydrogen (RHE) by the Nernst equation: $E_{VS.RHE} = E_{VS.Ag/AgCl} + 0.059pH + E^{\theta}_{Ag/AgCl}$. All the resulting potentials without IR-corrected. Had been activated with e adequate cyclic voltammetry (CV) before all electrochemical tests. The linear sweep voltammetry (LSV) is obtained with a scanning rate of 1mV s^{-1} reaching a steady-state to minimize experimental error. Electrochemical impedance spectroscopy (EIS) was processed from 100 kHz to 10 mHz with 5 mV ac amplitude. transform Polarization curve by a simplified formula ($\eta = a + b \log j$)), where b defines the Tafel slope. The electrochemical capacitance in the range of non-faraday (1.1307-1.1707 V vs. RHE for OER, 1.0087-1.0587 V vs. RHE for HER) was conducted by CV with a series of scanning rates (eg.: 100, 80, 60, 40, and 20 mV s^{-1}) to calculate the double layer capacitance which can estimate the electrochemical surface area. For comparison, the CFP (1*1 cm^2) coated with commercial catalyst (20 wt% Pt/C and RuO_2) in the same amount of mass loading as the NiCoP@NiFeP was considered as cathode and anode electrode, respectively. The stability was assessed by the Multi-Current Steps method.

An AEM (MTR-1 Tianjin GAOSSUNION PHOTOELECTRIC Technology Co., Ltd. China), which consists of a current collector, MEA type reactor (serpentine channel), Anion exchange membrane (Fuma FAA-PK-130), working electrodes (NiCoP@NiFeP). For comparison, the CFP (1*1 cm^2) coated with commercial catalyst (20 wt% Pt/C and RuO_2) in the same amount of mass loading (1.1 mg cm^{-2}) as the NiCoP@NiFeP was considered as cathode and anode electrode, respectively. All the AEM resulting potentials with 90% IR-corrected (R_{corr} 0.5 Ω).

S1 The SEM images of different ratio of NiCo:NiFe in NiCo@NiFe Pre and the corresponding phosphates

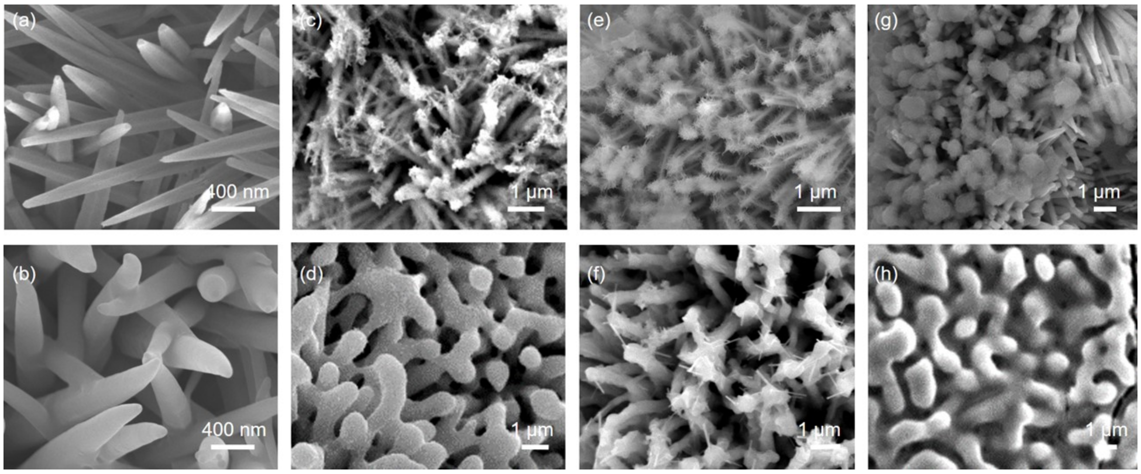

Fig. S1 SEM images of (a-b) NiCo NRs and NiCoP; (c-d) the ratio of NiCo:NiFe in NiCo@NiFe Pre less than 1 and the corresponding phosphates ; (c) the ratio of NiCo:NiFe in NiCo@NiFe Pre is about 1 and the corresponding phosphates (d) the ratio of NiCo:NiFe in NiCo@NiFe Pre is larger than 1 and the corresponding phosphates.

S2 XRD pattern of samples

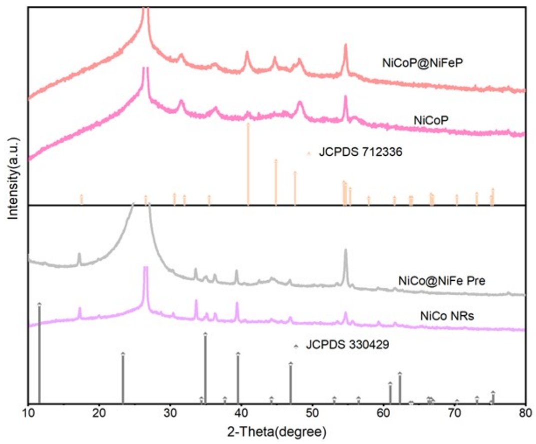

Fig. S2. XRD pattern of NiCo NRs, NiCo@NiFe precursors, NiCoP, and NiCoP@NiFeP.

S3 XRD pattern of NiFe NRs and NiFeP

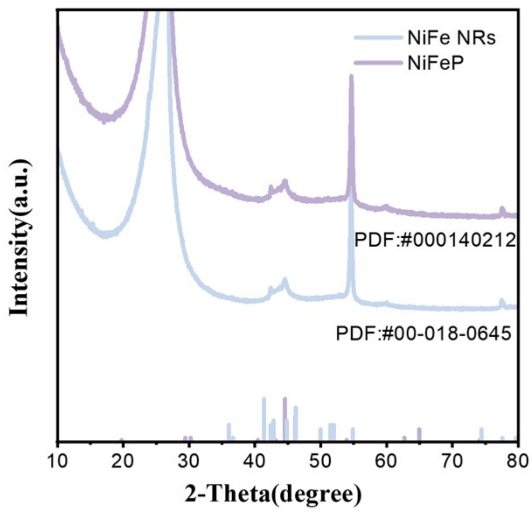

Fig. S3. XRD pattern of NiFe NRs and NiFeP.

S4 The SEM images of samples

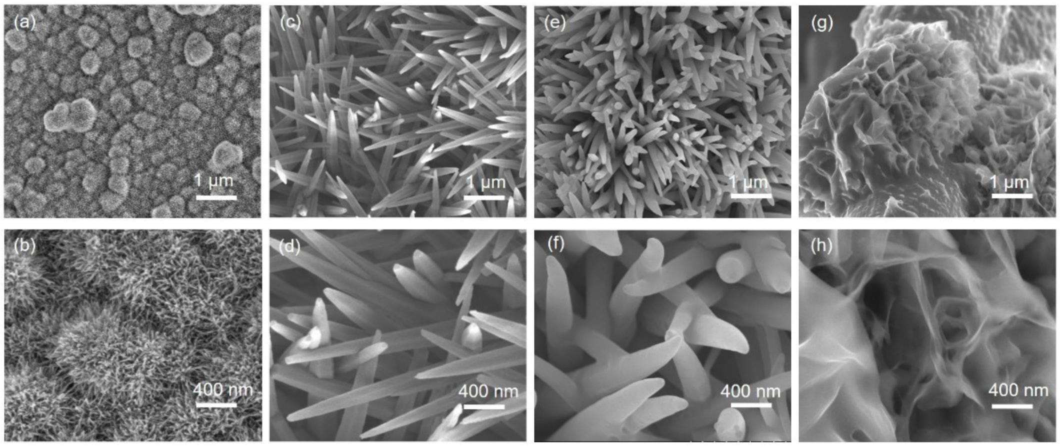

Fig. S4. SEM images of (a-b) NiFe NRs; (c-d) NiCo NRs; (e-f) NiCoP/CFP; and (g-h) NiFeP/CFP at different magnifications.

S5 XPS pattern of NiFeP@ NiCoP and NiFeP

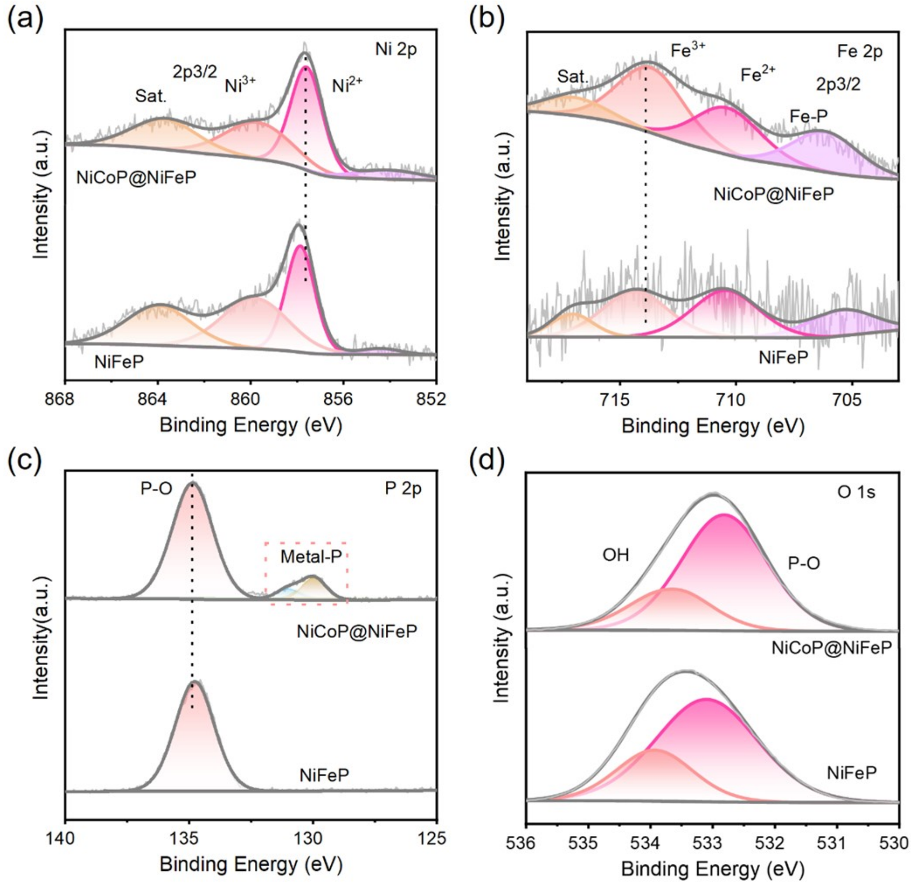

Fig. S5. XPS spectra of NiCoP@NiFeP /CFP and NiFeP/CFP. (a) Ni 2p; (c) Fe 2p ;(d) P 2p; (f) O 1s.

The XPS spectra of NiFeP were supplied in **Figure S5**. The Fe 2p3/2 peaks of NiFeP at 705.6, 710.80 and 714.2 eV corresponds to the Fe-P bonding, Fe^{2+}, and Fe^{3+} characteristic peaks, respectively, whereas the other shakeup satellite peak distributed at around 717.2 eV. Comparing with the XPS spectra of NiFeP and NiCoP@NiFeP, we can clearly see that the $Fe2p_{3/2}$ of NiFeP obviously has a positive shift, while the peak position of the P 2p shows a negative shift, indicating an increased electronic density for P, suggesting the more pronounced electron tra the inte nsfer in NiCoP@NiFeP due to raction between NiFeP and NiCoP in the closely contacted heterointerface (*Adv. Energy Mater.* 2019, 9, 1901213; *J. Mater. Chem. A*, 2021,9, 18421-18430). The XPS spectra in accordance with the DFT results that NiCoP@NiFeP moderate quantity of electrons, which owns ideal hydrogen adsorption energy. The following was replenished in the revised manuscript.

S6 The polarization of different ratio of NiCo:NiFe in NiCo@NiFe Pre and the corresponding phosphates

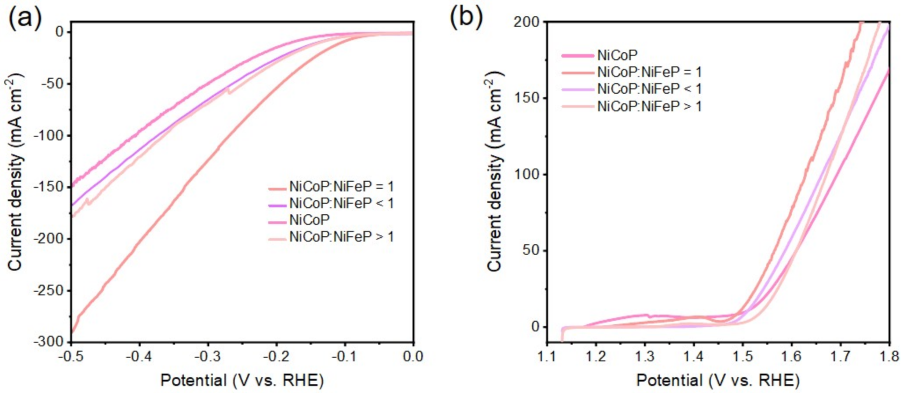

Fig. S6 (a) The HER polarization curves of the different ratio of NiCoP and NiFeP samples in 1.0 M KOH solution

(b) The OER polarization curves of the different ratio of NiCoP and NiFeP samples in 1.0 M KOH solution.

S7 The equivalent circuit diagram of EIS

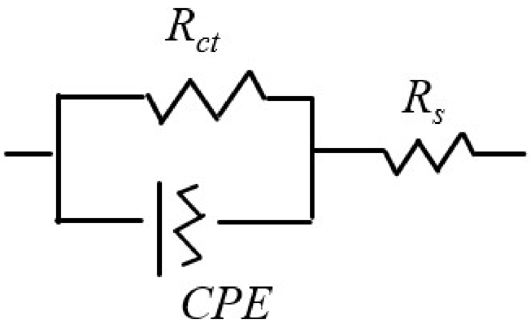

Fig. S7. the Randles circuit equivalent circuit diagram.

S8 Cyclic voltammetry (CV) curves of HER

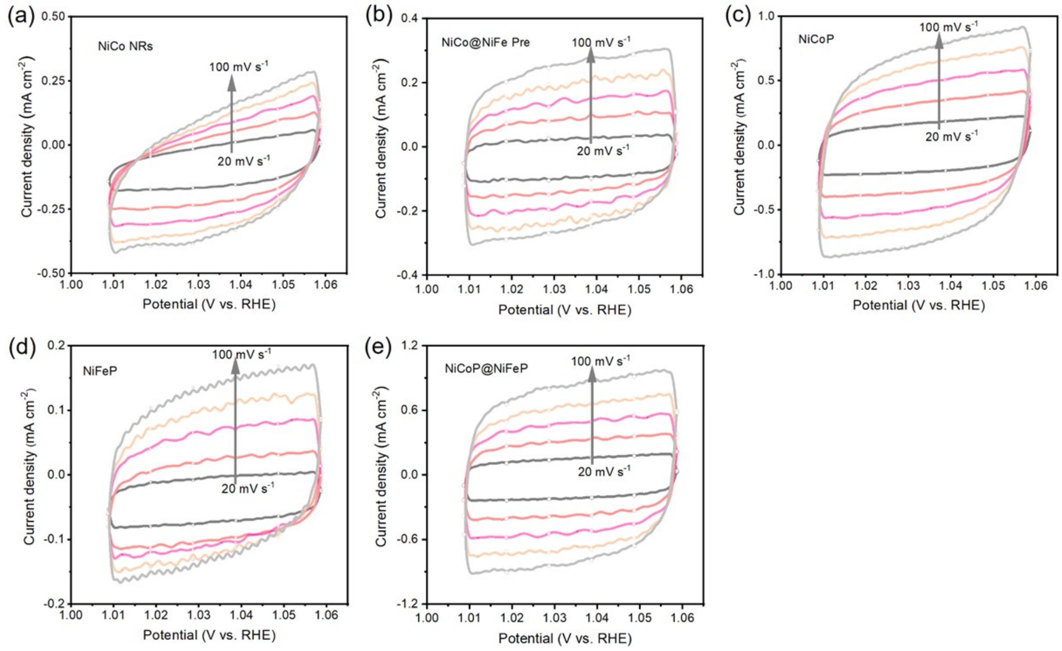

Fig. S8. Cyclic Volta photograms in the region of 1.0087-1.0587 V vs. RHE for (a) NiCo NRs /CFP; (b) NiCo@NiFe precursors /CFP; (c) NiCoP/CFP; (d) NiFeP/CFP; and (e) NiCoP@NiFeP/CFP at various scan rates (20, 40, 60 mV s^{-1} etc.).

S9 The crystal structures of samples

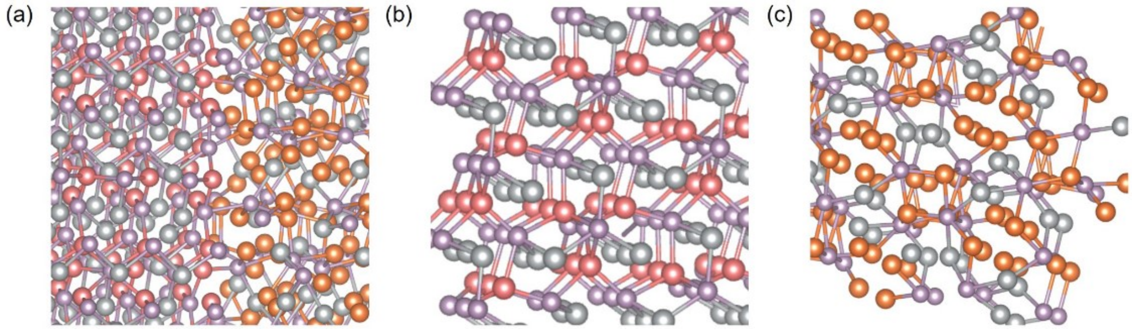

Fig. S9. (a)-(c) density of states of NiCoP@NiFeP, NiCoP, and NiFeP systems.

S10. Digital images of the wetting process of 1.0 M KOH droplets

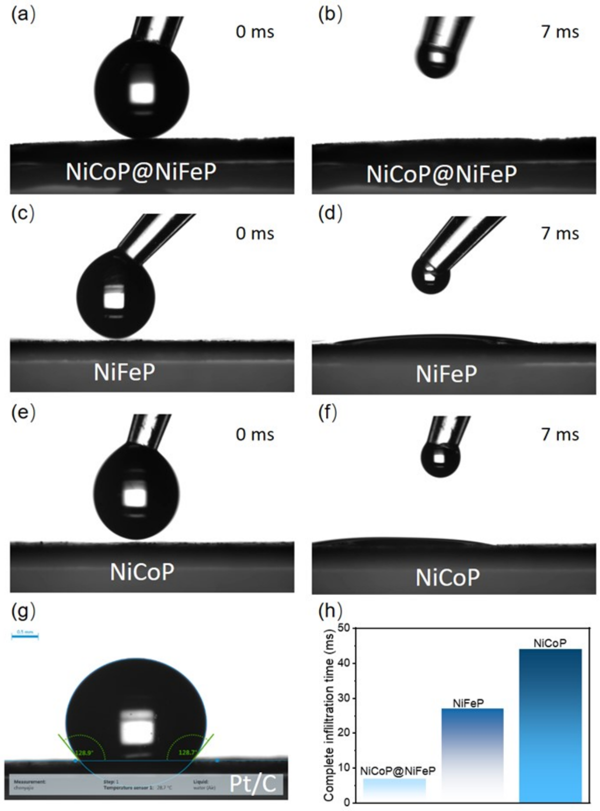

Fig. S10. Digital images of the wetting process of 1.0 M KOH droplets for (a-b) NiCoP@NiFeP; (c-d) NiFeP/CFP; (e-f) NiCoP/CFP; and (g) Pt/C., and (h) the complete infiltration time.

S11. The Faradaic efficiency OER and HER

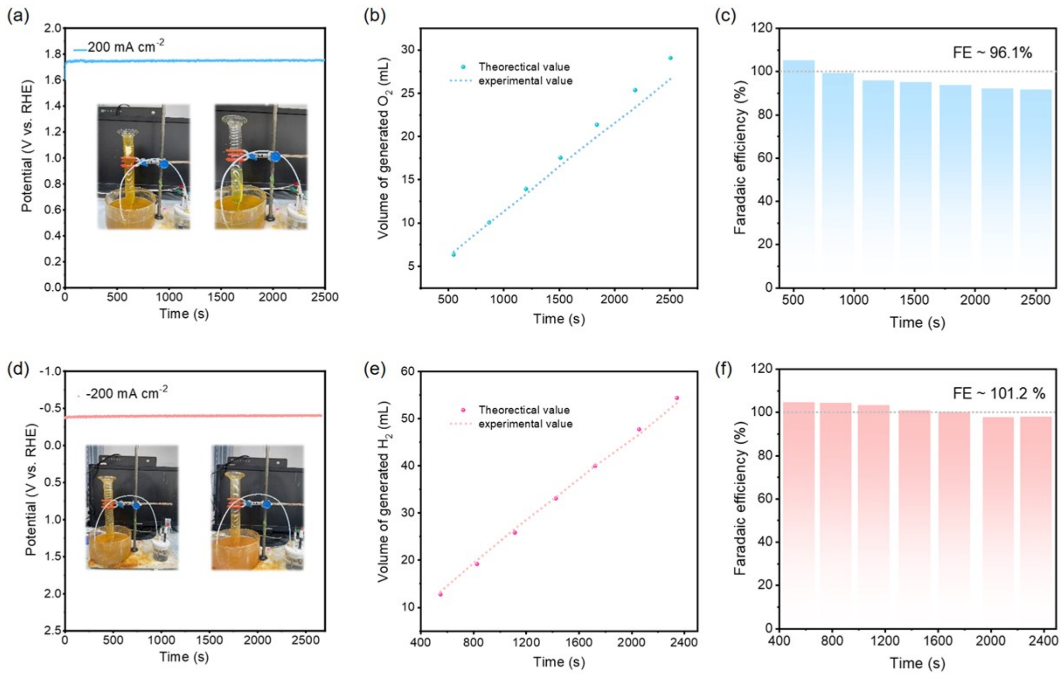

Fig. S11. (a) Time-dependent current density curves of NiCoP@NiFeP, with the inset showing the photograph of the measure setup via drainage gas gathering method. (b) Time-dependent O_2 yield and the theoretical value, and (c) the calculated Faradaic efficiency in OER; (d) Time-dependent current density curves of NiCoP@NiFeP (e) Time-dependent H_2 yield and the theoretical value, and (f) the calculated Faradaic efficiency in HER.

S12 Cyclic voltammetry (CV) curves of OER

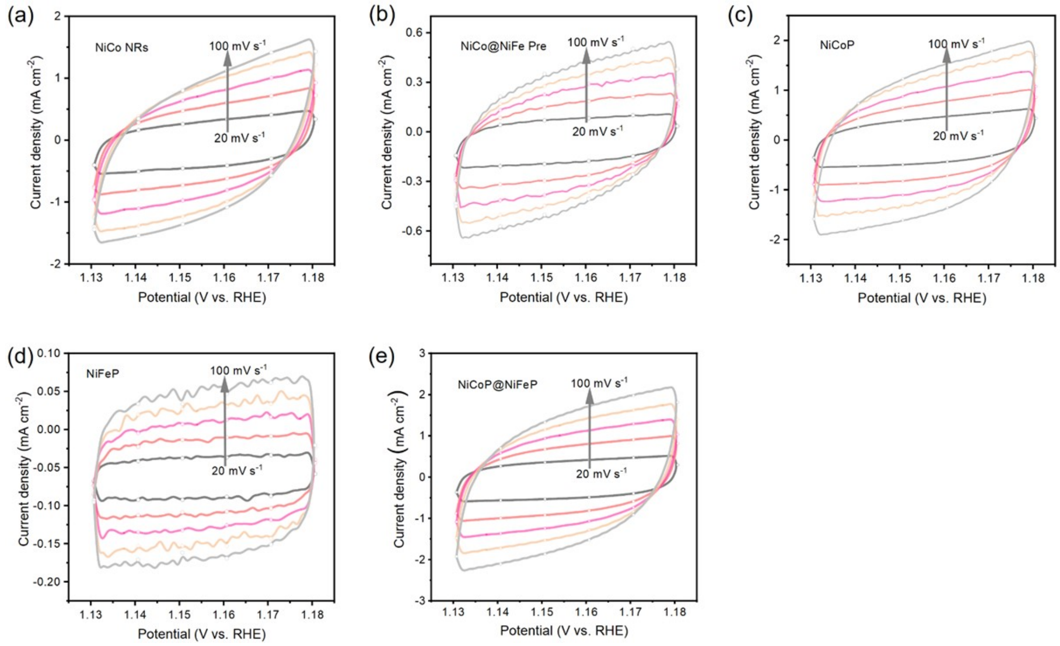

Fig. S12. Cyclic Volta photograms in the region of 1.1307-1.1807 V vs. RHE for (a)NiCo NRs /CFP, (b) NiCo@NiFe precursors /CFP, (c) NiCoP/CFP, (d) NiFeP/CFP, and (e) NiCoP@NiFeP/CFP at various scan rates (20, 40, 60 mV s^{-1} etc.).

S13 XRD patterns of NiCoP@NiFeP before and after HER/OER test

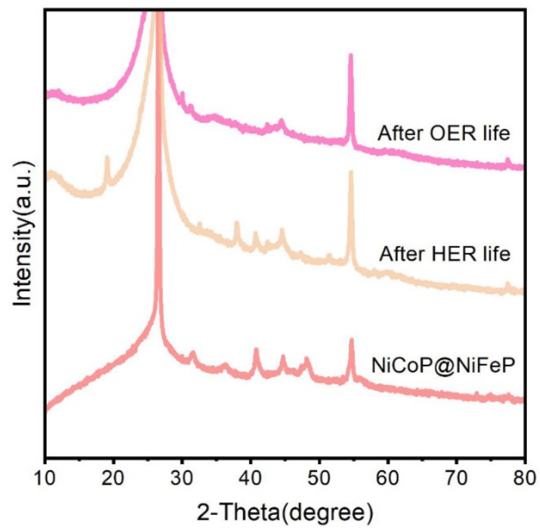

Fig. S13. XRD pattern of NiCoP@NiFeP after the Multi-Current Steps testing for overall water splitting.

S14 SEM images of NiCoP@NiFeP after HER/OER test

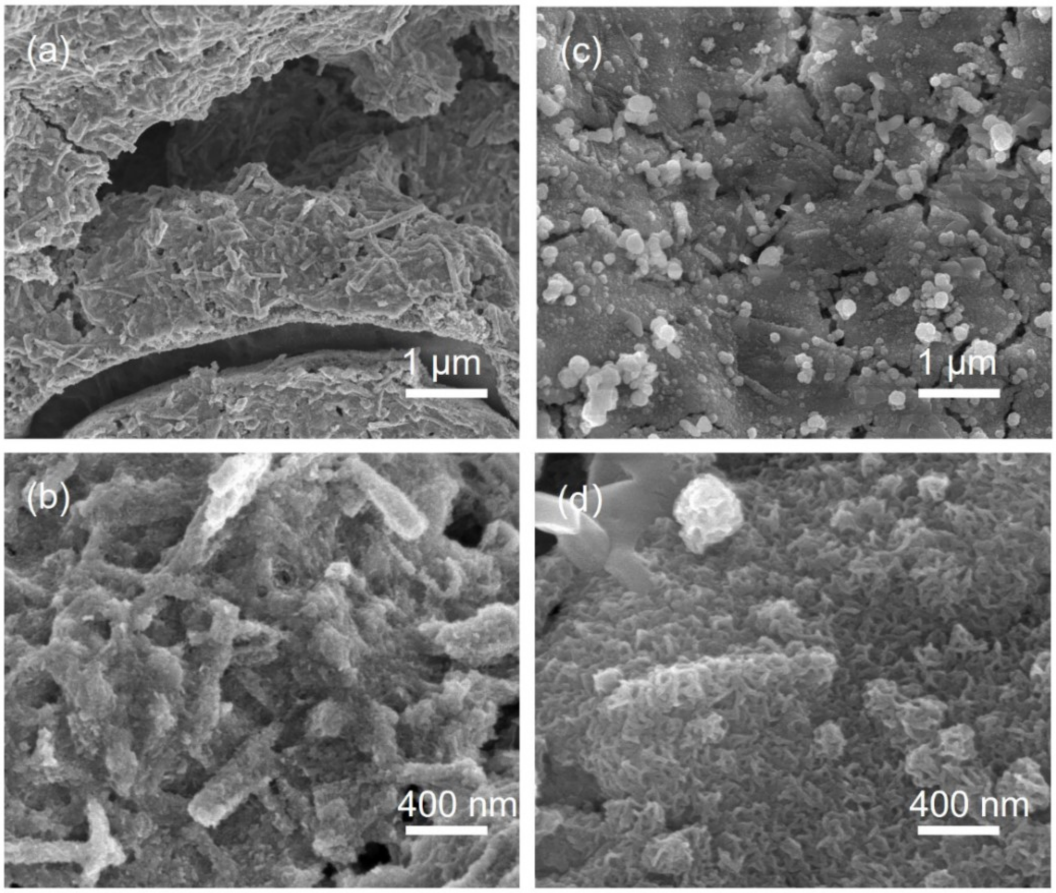

Fig. S14. SEM images of NiCoP@NiFeP(a-b) of the HER, (c-d) of the OER after the Multi-Current Steps testing for overall water splitting.

S15 XPS spectras of NiCoP@NiFeP after HER/OER test

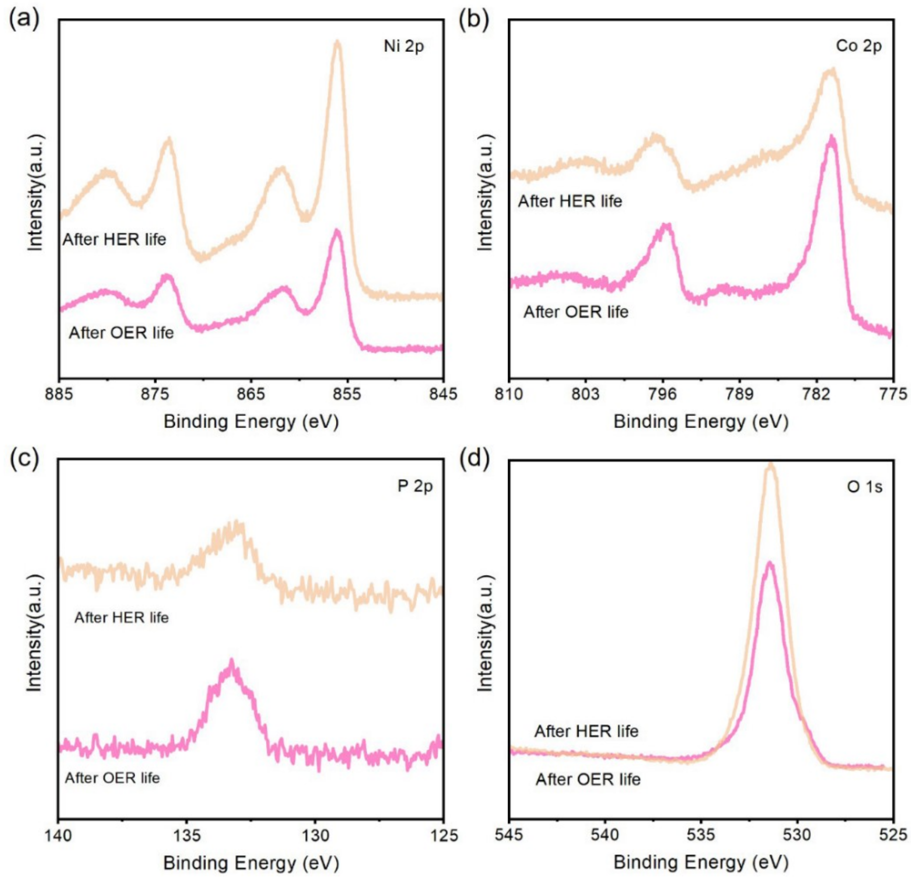

Fig. S15. XPS spectra (a) Ni 2p, (b) Co 2p, (c)P 2p, (d) O1s of NiCoP@NiFeP after the step-chronopotentiometric testing for overall water splitting.

S16 Cyclic voltammetry (CV) curves

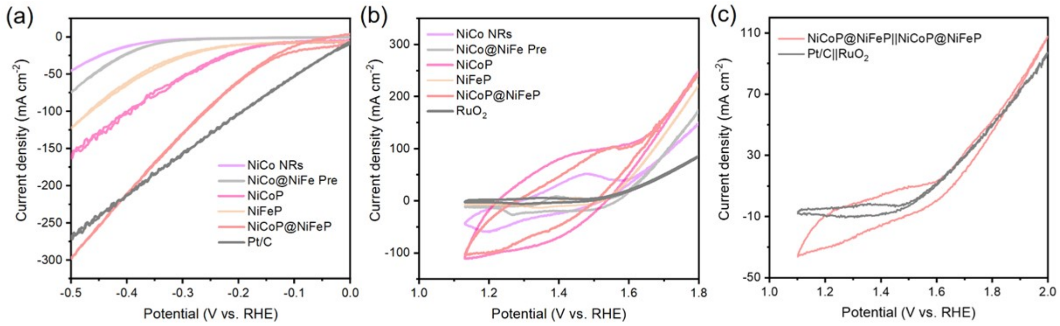

Fig. S16. Polarization curves (without iR compensation) (a) of the HER, (b) of the OER, (c) of the water electrolyzer with NiCoP@NiFeP || NiCoP@NiFeP and Pt/C || RuO_2 for overall water splitting.

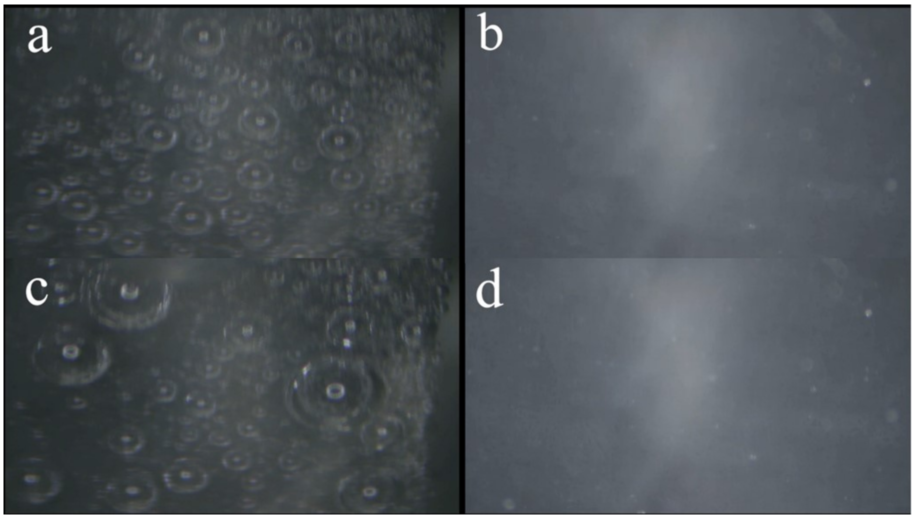

Movie S1. The movie of HER process of the (a)-(c) NiCoP@NiFeP, (b)-(d) Pt/Cat 50 and 200 mA cm^{-2}

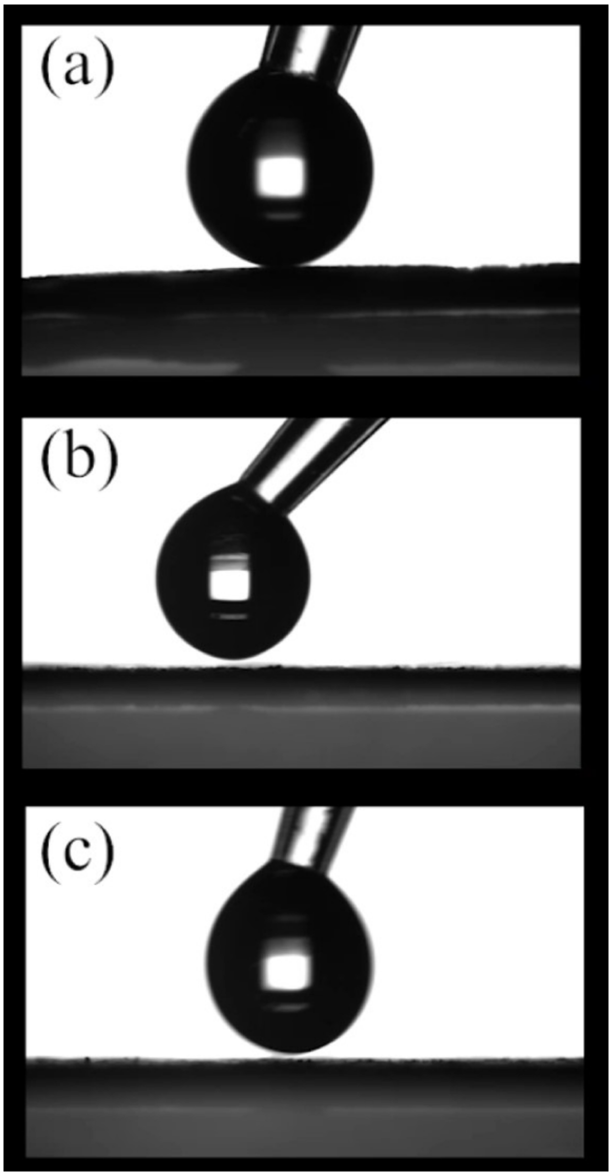

Movie S2.The movie of of the wetting process of 1.0 M KOH droplets for (a-b) NiCoP@NiFeP; (c-d) NiFeP/CFP; (e-f) NiCoP/CFP

Table S1. Recent reported HER catalytic activity in alkaline electrolytes. (**η_{10}** is the abbreviative of η (mV) at 10 mA cm^{-2})

Catalyst	η_{10}	Ref.	Catalyst	η_{10}	Ref.
NiCoP@NiFeP	**98**	**this work**	NiCoP/NPC	128	ref.S19 [19]
CoFe PBA@CoP	100	ref.S1 [1]	NiCoP/CoP-Ti_4O_7	128	ref.S20 [20]
Mo-$NiCo_2O_4$/$Co_{5.47}$N/NF	100	ref.S2 [2]	Ni_2P-Fe_2P	128	ref.S21 [21]
$CoS_{1-x}P_x$	101	ref.S3 [3]	Fe-Ni_3S_2/Ni_2P@C/NF	129	ref.S22 [22]
S-NiCoP NW/CFP	102	ref.S4 [4]	NiFeP/CC	129	ref.S23 [23]
NiCoP-NWAs/NF	104	ref.S5 [5]	(Ni, Fe)S_2@MoS_2	130	ref.S24 [24]
CoS_x-Ni_3S_2/NF	105	ref.S6 [6]	NiFe-LDH@CoS_x	136	ref.S25 [25]
FeOOH/Ni_3S_2/NF	106	ref.S7 [7]	CoP@FeCoP	141	ref.S26 [26]
Mo-Ni_3S_2/Ni_xP_y/NF	109	ref.S8 [8]	Co/CoO@NC@CC	152	ref.S27 [27]
$NiCo_{1.6}P$ alloy coating	112	ref.S9 [9]	3D NiFe LDH-POM	156	ref.S28 [28]
$FeNi_2P$@PC/CuxS	112	ref.S10[10]	Cu-(a-$NiSe_x$/c-$NiSe_2$)/TiO_2	156.9	ref.S29 [29]
Fe-Ni phosphide	116	ref.S11[11]	CoP-InNC@CNT	159	ref.S30 [30]
Co-Ni-P/MoS_2	116	ref.S12[12]	Co@Co-P@NPCNTs	160	ref.S31 [31]
NiFeLDH@NiCoP/NF	120	ref.S13[13]	porous Ni_2P nanosheets	168	ref.S32 [32]

CoP/NiCoP	121	ref.S14[14]	PrGO/NiCoP	169	ref.S33 [33]

Table S1 Continued.

Catalyst	**η_{10}**	**Ref.**	**Catalyst**	**η_{10}**	**Ref.**
$(Ni_xFe_{1-x})_2P$	125	ref.S15[15]	Co-Fe oxyphosphide microtubes	180	ref.S34[34]
FeNiP/NPCS	126	ref.S16[16]	Cu_3N@CoNiCHs@CF	182	ref.S35[35]
NiCoP-150	127	ref.S17[17]	Fe-Ni_5P_4/NiFeOH	197	ref.S36 [36]
MXene-NiCoP	127	ref.S18[18]	/	/	/

Table S2 Rct value in HER and OER process

Samples	R_{ct} value in HER process	R_{ct} value in OER process
NiCoP@NiFeP	2.61 Ω	1.79 Ω
NiCoP	3.02 Ω	5.11 Ω
NiFeP	12.0 Ω	2.94 Ω
NiCo NRs	3.33 Ω	2.96 Ω
NiCo@NiFe Pre	5.95 Ω	2.19 Ω
Pt/C	1.01 Ω	--
RuO_2	--	4.11 Ω

Table S3. Recent reported OER catalytic activity in alkaline electrolytes.

Catalysts	OER performance in alkaline condition			Reference
	η (mV) at 10 mA cm^{-2};	η (mV) at 50 mA cm^{-2};	η (mV) at 100 mA cm^{-2};	
NiCoP@NiFeP	**256**	**300**	**330**	**this work**
$Co_xFe_{1-x}P$	277	305	/	ref.S37 [37]
NiCoP	242	305	330	ref.S38 [38]
NiCoP/C@FeOOH	271	321	340	ref.S39 [39]
Ni/NiCoP	260	300	345	ref.S40 [40]
Mo-NiCoP	269	328	364	ref.S41[41]
NiFeVP	234	320	352	ref.S42 [42]
3DP GC/NiFeP	180	255	340	ref.S43 [43]
NiFeP-WO_x	270	330	352	ref.S44 [44]
NiCoP	/	308	332	ref.S45 [45]
Co_{12}@Ni_3S_2/NF	/	358	420	ref.S46 [46]
Fe-NiCoP/PBA HNCs	290	/	/	ref.S47 [47]
N-$NiCoP_x$/NCF	298	/	/	ref.S48 [48]
$Ni_{2-x}Ru_xP$	340	/	/	ref.S49 [49]
CoP/TiO_x	330	380	420	ref.S50 [50]
CoFe/SNC	308	/	/	ref.S51 [51]
$NiCo_2O_4$/NCNTs/NiCo	350	/	/	ref.S52 [52]
NiFe(O_{xy})Hydroxides	270	/	/	ref.S53 [53]
NiFeP/MXene	286	/	/	ref.S54 [54]

Table S4. Recent reported overall water splitting catalytic activity in alkaline electrolytes.

Catalysts	Water splitting performance in alkaline condition		Reference
	Current density (mA cm^{-2})	Cell voltage (V)	
NiCoP@NiFeP	**1000**	**1.93**	**this work**
Pt/C|| RuO_2	1000	2.42	**this work**
Ni_3N/Ni||Ti-mesh	500	1.9	ref.S55 [55]
NiCoP(+)||NiCoP(-)	1000	2.37	ref.S56 [56]
Ta-TaS_2||IrO_2	1000	1.98	ref.S57 [57]
NCCu	500	2.02	ref.S58 [58]
Pt/C/$(NiCo)_3Se_4$	1000	2	ref.S59[59]
$NiS_{0.5}Se_{0.5}$	350	1.98	ref.S60 [60]
Co_4N-CeO_2	1000	2.28	ref.S61 [61]
Ru-CoOx/NF	1000	2.2	ref.S62 [62]
Fe-FVO-60-act	1000	2	ref.S63 [63]
3D PNi	600	2.56	ref.S64 [64]
S-(Ni,Fe)OOH	1000	1.951	ref.S65 [65]
NiFe(OH)x/FeS/IF|| MoNi4/MoO_2/NF	300	1.95	ref.S66 [66]

1 L. Quan, S. H. Li, Z. P. Zhao, J. Q. Liu, Y. Ran, J. Y. Cui, W. Lin, X. L. Yu, L. Wang, Y. H. Zhang and J. H. Ye, *Small Methods*, 2021, **5**, 2100125.
2 W. X. Liu, L. H. Yu, R. L. Yin, X. L. Xu, J. X. Feng, X. Jiang, D. Zheng, X. L. Gao, X. B. Gao, W. B. Que, P. C. Ruan, F. F. Wu, W. H. Shi and X. H. Cao, *Small*, 2020, **16**, 1906775.
3 R. Boppella, J. Park, H. Lee, G. Jang and J. Moon, *Small Methods*, 2020, **4**, 2000043.
4 Y. Y. Qi, L. Zhang, L. Sun, G. J. Chen, Q. M. Luo, H. Q. Xin, J. H. Peng, Y. Li and F. Ma, *Nanoscale*, 2020, **12**, 1985-1993.
5 J. Z. Li, G. D. Wei, Y. K. Zhu, Y. L. Xi, X. X. Pan, Y. Ji, I. V. Zatovsky and W. Han, *J. Mater. Chem. A.*, 2017, **5**, 14828-14837.
6 L. W. Jiang, N. Yang, C. X. Yang, X. Y. Zhu, Y. N. Jiang, X. P. Shen, C. C. Li and Q. F. Sun, *Appl. Catal., B*, 2020, **269**, 118780.
7 X. F. Ji, C. Q. Cheng, Z. H. Zang, L. L. Li, X. Li, Y. H. Cheng, X. J. Yang, X. F. Yu, Z. M. Lu, X. H. Zhang and H. Liu, *J. Mater. Chem. A.*, 2020, **8**, 21199-21207.
8 X. Luo, P. X. Ji, P. Y. Wang, R. L. Cheng, D. Chen, C. Lin, J. N. Zhang, J. W. He, Z. H. Shi, N. Li, S. Q. Xiao and S. C. Mu, *Adv. Mater.* , 2020, **10**, 1903891.
9 V. S. Sumi, M. A. Sha, S. R. Arunima and S. M. A. Shibli, *Electrochim. Acta*, 2019, **303**, 67-77.
10 D. T. Tran, H. T. Le, V. H. Hoa, N. H. Kim and J. H. Lee, *Nano Energy*, 2021, **84**, 105861.
11 Y. H. Wu, Y. Y. Yi, Z. T. Sun, H. Sun, T. Q. Guo, M. H. Zhang, L. F. Cui, K. Jiang, Y. Peng and J. Y. Sun, *Chem. Eng. J.* , 2020, **390**, 124515.
12 J. H. Bao, Y. M. Zhou, Y. W. Zhang, X. L. Sheng, Y. Y. Wang, S. Liang, C. Guo, W. Yang, T. Zhuang and Y. J. Hu, *J. Mater. Chem. A.*, 2020, **8**, 22181-22190.
13 H. J. Zhang, X. P. Li, A. Hähnel, V. Naumann, C. Lin, S. Azimi, S. L. Schweizer, A. W. Maijenburg and R. B. Wehrspohn, *Adv. Funct. Mater.* , 2018, **28**, 1706847.
14 X. P. Liu, S. F. Deng, D. D. Xiao, M. X. Gong, J. N. Liang, T. H. Zhao, T. Shen and D. L. Wang, *Adv. Funct. Mater.* , 2019, **11**, 42233-42242.
15 S.-F. Sun, X. Zhou, B. W. Cong, W. Z. Hong and G. Chen, *ACS Catal.* , 2020, **10**, 9086-9097.
16 J.-T. Ren, Y.-S. Wang, L. Chen, L.-J. Gao, W.-W. Tian and Z.-Y. Yuan, *Chem. Eng. J.* , 2020, **389**, 124408.
17 X. P. Liu, S. F. Deng, P. F. Liu, J. N. Liang, M. X. Gong, C. L. Lai, Y. Lu, T. H. Zhao and D. L. Wang, *Sci. Bull.*, 2019, **64**, 1675-1684.
18 Q. Yue, J. Sun, S. Chen, Y. Zhou, H. J. Li, Y. Chen, R. Zhang, G. Wei and Y. J. Kang, *ACS Appl. Mater. Interfaces* 2020, **12**, 18570-18577.
19 M. J. Yi, B. B. Lu, X. T. Zhang, Y. B. Tan, Z. Y. Zhu, Z. C. Pan and J. H. Zhang, *Appl. Catal., B*, 2021, **283**, 119635.
20 D. Ma, R. H. Li, Z. L. Zheng, Z. J. Jia, K. Meng, Y. Wang, G. M. Zhu, H. Zhang and T. Qi, *ACS Sustainable Chem. Eng.*, 2018, **6**, 14275-14282.
21 L. B. Wu, L. Yu, F. H. Zhang, B. McElhenny, D. Luo, A. Karim, S. Chen and Z. F. Ren, *Adv. Funct. Mater.* , 2020, **31**, 2006484.
22 W.-Z. Chen, P.-Y. Liu, L. Zhang, Y. Liu, Z. L. Liu, J. He and Y.-Q. Wang, *Chem. Eng. J.* , 2021, **424**, 130434.
23 S. Wang, J. G. Cai, C. Lv, C. Hu, H. T. Guan, J. Q. Wang, Y. Shi, J. F. Song, A. Watanabe and X. B. Ge, *Chem. Eng. J.* , 2021, **420**, 129972.
24 Y. K. Liu, S. Jiang, S. J. Li, L. Zhou, Z. H. Li, J. M. Li and M. F. Shao, *Appl. Catal., B*, 2019, **247**, 107-114.
25 Y. Yang, Y. C. Xie, Z. H. Yu, S. S. Guo, M. W. Yuan, H. Q. Yao, Z. P. Liang, Y. R. Lu, T.-S. Chan, C. Li, H. L. Dong and S. L. Ma, *Chem. Eng. J.* , 2021, **419**, 129512.
26 J. H. Shi, F. Qiu, W. B. Yuan, M. M. Guo and Z.-H. Lu, *Chem. Eng. J.* , 2021, **403**, 126312.
27 K. Q. Dai, N. Zhang, L. L. Zhang, L. X. Yin, Y. F. Zhao and B. Zhang, *Chem. Eng. J.* , 2021, **414**,

128804.
28 C. L. Li, Z. J. Zhang and R. Liu, *Small*, 2020, **16**, e2003777.
29 K. R. Park, D. T. Tran, T. T. Nguyen, N. H. Kim and J. H. Lee, *Chem. Eng. J.* , 2021, **422**, 130048.
30 L. L. Chai, Z. Y. Hu, X. Wang, Y. W. Xu, L. J. Zhang, T.-T. Li, Y. Hu, J. J. Qian and S. M. Huang, *Adv. Sci.* , 2020, **7**, 1903195.
31 J. Q. Jiao, W. J. Yang, Y. Pan, C. Zhang, S. J. Liu, C. Chen and D. S. Wang, *Small*, 2020, **16**, 2002124.
32 Q. Wang, Z. Q. Liu, H. Y. Zhao, H. Huang, H. Jiao and Y. P. Du, *J. Mater. Chem. A.*, 2018, **6**, 18720-18727.
33 T. Dong, X. Zhang, P. Wang, H.-S. Chen and P. Yang, *Carbon*, 2019, **149**, 222-233.
34 P. Zhang, X. F. Lu, J. w. Nai, S.-Q. Zang and X. W. Lou, *Adv. Sci.* , 2019, **6**, 1900576.
35 S.-Q. Liu, M.-R. Gao, S. B. Liu and J.-L. Luo, *Appl. Catal., B*, 2021, **292**, 120148.
36 C.-F. Li, J.-W. Zhao, L.-J. Xie, J.-Q. Wu and G.-R. Li, *Appl. Catal., B*, 2021, **291**, 119987.
37 S. Yue, S. S. Wang, Q. Z. Jiao, X. T. Feng, K. Zhan, Y. Q. Dai, C. H. Feng, H. S. Li, T. Y. Feng and Y. Zhao, *ChemSusChem*, 2019, **12**, 4461-4470.
38 C. Du, L. Yang, F. L. Yang, G. Z. Cheng and W. Luo, *ACS Catal.* , 2017, **7**, 4131-4137.
39 J.-G. Li, Y. Gu, H. C. Sun, L. Lv, Z. S. Li, X. Ao, X. Y. Xue, G. Hong and C. D. Wang, *Nanoscale*, 2019, **11**, 19959-19968.
40 Y. Lin, Y. Pan, S. J. Liu, K. A. Sun, Y. S. Cheng, M. Liu, Z. J. Wang, X. Y. Li and J. Zhang, *Appl. Catal., B*, 2019, **259**, 118039.
41 J. H. Lin, Y. T. Yan, C. Li, X. Q. Si, H. H. Wang, J. L. Qi, J. Cao, Z. X. Zhong, W. D. Fei and J. C. Feng, *Nano-Micro Lett.*, 2019, **11**, 55.
42 Y. Jeung, H. Jung, D. Kim, H. Roh, C. Lim, J. W. Han and K. Yong, *J. Mater. Chem. A.*, 2021, **9**, 12203-12213.
43 M. W. Peng, D. L. Shi, Y. H. Sun, J. Cheng, B. Zhao, Y. M. Xie, J. C. Zhang, W. Guo, Z. Jia, Z. Q. Liang and L. Jiang, *Adv. Mater.* , 2020, **32**, 1908201.
44 D. Kim, Y. Jeong, H. Roh, C. Lim and K. Yong, *J. Mater. Chem. A.*, 2021, **9**, 10909-10920.
45 Y. J. Li, H. C. Zhang, M. Jiang, Y. Kuang, X. M. Sun and X. Duan, *Nano Res.*, 2016, **9**, 2251-2259.
46 X. Tong, Y. Li, N. Pang, Y. H. Qu, C. H. Yan, D. Y. Xiong, S. H. Xu, L. W. Wang and P. K. Chu, *Chem. Eng. J.* , 2021, **425**, 130455.
47 D. Li, C. C. Liu, W. X. Ma, S. J. Xu, Y. K. Lu, W. X. Wei, J. J. Zhu and D. L. Jiang, *Electrochim. Acta*, 2021, **367**, 137492.
48 R. X. Jin, J. Huang, G. L. Chen, W. Chen, B. Ouyang, D. L. Chen, E. Kan, H. Zhu, C. R. Li, D. Z. Yang and K. Ostrikov, *Chem. Eng. J.* , 2020, **402**, 126257.
49 D. R. Liyanage, D. Li, Q. B. Cheek, H. Baydoun and S. L. Brock, *J. Mater. Chem. A.*, 2017, **5**, 17609-17618.
50 Z. Liang, W. Zhou, S. Gao, R. Zhao, H. J. Zhang, Y. Tang, J. Cheng, T. Qiu, B. Zhu, C. Qu, W. Guo, Q. Wang and R. Zou, *Small*, 2020, **16**, 1905075.
51 C. H. Li, E. H. Zhou, Z. Y. Yu, H. X. Liu and M. Xiong, *Appl. Catal., B*, 2020, **269**, 118771.
52 C. Chen, H. Su, L.-N. Lu, Y.-S. Hong, Y. Z. Chen, K. Xiao, T. Ouyang, Y. L. Qin and Z.-Q. Liu, *Chem. Eng. J.* , 2021, **408**, 127814.
53 T. Y. Wang, G. Nam, Y. Jin, X. Y. Wang, P. J. Ren, M. G. Kim, J. S. Liang, X. D. Wen, H. Jang, J. Han, Y. H. Huang, Q. Li and J. Cho, *Adv. Mater.* , 2018, **30**, 1800757.
54 J. X. Chen, Q. W. Long, K. Xiao, T. Ouyang, N. Li, S. Y. Ye and Z.-Q. Liu, *Sci. Bull.*, 2021, **66**, 1063-1072.
55 D. Zhang, H. Li, A. Riaz, A. Sharma, W. Liang, Y. Wang, H. Chen, K. Vora, D. Yan, Z. Su, A.

Tricoli, C. Zhao, F. J. Beck, K. Reuter, K. Catchpole and S. Karuturi, *Energy Environ. Sci.*, 2021, DOI: 10.1039/d1ee02013g.
56 H. Liang, A. N. Gandi, D. H. Anjum, X. Wang, U. Schwingenschlogl and H. N. Alshareef, *Nano Lett.*, 2016, **16**, 7718-7725.
57 Q. Yu, Z. Zhang, S. Qiu, Y. Luo, Z. Liu, F. Yang, H. Liu, S. Ge, X. Zou, B. Ding, W. Ren, H. M. Cheng, C. Sun and B. Liu, *Nat. Commun.*, 2021, **12**, 6051.
58 C. L. Huang, K. Sasaki, D. Senthil Raja, C. T. Hsieh, Y. J. Wu, J. T. Su, C. C. Cheng, P. Y. Cheng, S. H. Lin, Y. Choi and S. Y. Lu, *Adv. Energy Mater.* , 2021, DOI: 10.1002/aenm.202101827, 2101827.
59 J. Abed, S. Ahmadi, L. Laverdure, A. Abdellah, C. P. O'Brien, K. Cole, P. Sobrinho, D. Sinton, D. Higgins, N. J. Mosey, S. J. Thorpe and E. H. Sargent, *Adv. Mater.* , 2021, **33**, e2103812.
60 Y. Wang, X. Li, M. Zhang, Y. Zhou, D. Rao, C. Zhong, J. Zhang, X. Han, W. Hu, Y. Zhang, K. Zaghib, Y. Wang and Y. Deng, *Adv. Mater.* , 2020, **32**, e2000231.
61 H. Sun, C. Tian, G. Fan, J. Qi, Z. Liu, Z. Yan, F. Cheng, J. Chen, C. P. Li and M. Du, *Adv. Funct. Mater.* , 2020, **30**, 1910596.
62 D. Wu, D. Chen, J. Zhu and S. Mu, *Small*, 2021, **17**, e2102777.
63 F. Nur Indah Sari, S. Abdillah and J.-M. Ting, *Chem. Eng. J.* , 2021, **416**, 129165.
64 T. Kou, S. Wang, R. Shi, T. Zhang, S. Chiovoloni, J. Q. Lu, W. Chen, M. A. Worsley, B. C. Wood, S. E. Baker, E. B. Duoss, R. Wu, C. Zhu and Y. Li, *Adv. Energy Mater.* , 2020, **10**, 2002955.
65 L. Yu, L. Wu, B. McElhenny, S. Song, D. Luo, F. Zhang, Y. Yu, S. Chen and Z. Ren, *Energy Environ. Sci.*, 2020, **13**, 3439-3446.
66 S. Niu, W. J. Jiang, T. Tang, L. P. Yuan, H. Luo and J. S. Hu, *Adv. Funct. Mater.* , 2019, **29**, 1902180.